



**HAL**  
open science

## **Innovative photocatalytic reactor for the degradation of VOCs and microorganism under simulated indoor air conditions: Cu-Ag/TiO<sub>2</sub>-based optical fibers at a pilot scale**

W. Abou Saoud, Abdoulaye Kane, Pierre Le Cann, Anne Gérard, L. Lamaa, L. Peruchon, C. Brochier, A. Bouzaza, D. Wolbert, A.A. Assadi

### ► To cite this version:

W. Abou Saoud, Abdoulaye Kane, Pierre Le Cann, Anne Gérard, L. Lamaa, et al.. Innovative photocatalytic reactor for the degradation of VOCs and microorganism under simulated indoor air conditions: Cu-Ag/TiO<sub>2</sub>-based optical fibers at a pilot scale. Chemical Engineering Journal, 2021, 411, pp.128622. 10.1016/j.cej.2021.128622 . hal-03130493

**HAL Id: hal-03130493**

**<https://hal.science/hal-03130493>**

Submitted on 2 Mar 2021

**HAL** is a multi-disciplinary open access archive for the deposit and dissemination of scientific research documents, whether they are published or not. The documents may come from teaching and research institutions in France or abroad, or from public or private research centers.

L'archive ouverte pluridisciplinaire **HAL**, est destinée au dépôt et à la diffusion de documents scientifiques de niveau recherche, publiés ou non, émanant des établissements d'enseignement et de recherche français ou étrangers, des laboratoires publics ou privés.

**Innovative photocatalytic reactor for the degradation of VOCs and  
microorganism under simulated indoor air conditions: Cu-Ag/TiO<sub>2</sub>-based  
optical fibers at a pilot scale**

Wala Abou Saoud<sup>1</sup>, Abdoulaye Kane<sup>2</sup>, Pierre Le Cann<sup>3</sup>, Anne Gerard<sup>3</sup>, Lina Lamaa<sup>4</sup>,  
Laure Peruchon<sup>4</sup>, Cedric Brochier<sup>4</sup>, Abdelkrim Bouzaza<sup>1</sup>, Dominique Wolbert<sup>1</sup>,  
Aymen Amine Assadi<sup>1\*</sup>

<sup>1</sup> Univ Rennes, ENSCR, UMR 6226 CNRS, ENSCR-11, allée de Beaulieu, CS 508307-35708 Rennes, France.

<sup>2</sup> UniLaSalle-Ecole des Métiers de l'Environnement (UniLaSalle-EME), Campus de Ker Lann, avenue Robert Schuman Bruz, France.

<sup>3</sup> Univ Rennes, Inserm, EHESP, Irset (Institut de recherche en santé, environnement et travail) - UMR\_S 1085, F-35000 Rennes, France.

<sup>4</sup> Brochier Technologies, 90 Rue Frédéric Fays, 69100 Villeurbanne Lyon, France.

\* Corresponding authors. E-mail: [aymen.assadi@ensc-rennes.fr](mailto:aymen.assadi@ensc-rennes.fr) (A. Assadi); Tel.: +33 2 23 23 81 52.

## **Abstract**

This study deals with photocatalytic application for indoor air pollution remediation. Two target compounds were selected: Butane-2,3-dione (C<sub>4</sub>H<sub>6</sub>O<sub>2</sub>) and Heptan-2-one (C<sub>7</sub>H<sub>14</sub>O). *Escherichia coli* (*E. coli*) were used as bacteria strain. Photocatalytic removal of VOCs alone, *E. coli* alone and their mixture (VOCs/*E. coli*) were evaluated, at pilot scale. Indeed, a series of experiments were carried out in a continuous planar reactor using a novel photocatalyst/TiO<sub>2</sub> technology with metal wires e.g. Copper (Cu)/Silver (Ag)-woven in optical fiber. Effects of experimental conditions such as flow rate (2-12 m<sup>3</sup>.h<sup>-1</sup>), VOCs inlet concentration (5-20 mg.m<sup>-3</sup>) and humidity levels (5-70%) on removal efficiency were investigated to properly appraise the oxidation performance in real conditions. All textile fiber photo-catalysts

(TiO<sub>2</sub>, TiO<sub>2</sub>-Cu and TiO<sub>2</sub>-Ag) showed good photocatalytic activities towards C<sub>4</sub>H<sub>6</sub>O<sub>2</sub>/C<sub>7</sub>H<sub>14</sub>O removal. As for simultaneous application with VOCs and *E. coli*: (i) in terms of VOCs removal efficiency, the same trend of performance was observed compared to VOCs experiments alone: 63% of removal efficiency by TiO<sub>2</sub> alone, 46% by TiO<sub>2</sub>-Ag and 52% by TiO<sub>2</sub>-Cu, (ii) in terms of *E. coli* inactivation, only experiments with TiO<sub>2</sub>-Cu and TiO<sub>2</sub>-Ag revealed a good performance.

**Keywords:** Photocatalysis, Indoor air treatment, mixture (VOCs/*E. coli*), Cu-Ag/TiO<sub>2</sub>-based optical fibers, continuous reactor

## 1. Introduction

Indoor air contaminants (such as Volatile Organic Compounds, VOCs and Bacteria), generated from food processing and preparation [1], can cause serious risks to public health. Moreover, the indoor air of all public places (Food industry, Hospitals, libraries,) were in the range above highly contaminated according to European Commission classification and the most isolates are considered as potential candidates involved in the establishment of sick building syndromes and often associated with clinical manifestations like allergy, rhinitis, asthma and conjunctivitis [2]. This can be due to the bacteria, viruses, molds and pollens. Thus, attention must be given to control those environmental factors which favor the growth and multiplication of microbes in indoor environment of public places to preserve the health of users and workers. Therefore, bacterial inactivation and VOCs removal remained very important approach for health and safety reasons [3,4]. The promising advanced technologies (Table 1.), provide interesting solutions at low cost with good removal efficiencies such as photocatalysis [5,6], cold plasma with/without catalysis [7-9] and catalytic ozonation [10,11]. Among the Advanced Oxidation Processes

(AOPs), the photocatalytic removal in air pollution abatement including chemical and microbiological contaminants, have been investigated by many researchers in recent years [12,13]. As a result, TiO<sub>2</sub>/UV-light oxidation was considered as a clean process for VOCs degradation with higher performance and complete mineralization [14-18]. Innovative catalysts can be used for increasing bacterial inactivation and VOCs degradation: Antibacterial metals such as Ag and Cu [19-22] coatings on semiconductors, usually titanium dioxide (TiO<sub>2</sub>), on glass fiber tissue [23-26], cellulosic paper [17] and polymer support [27] have been studied for indoor air treatment

The Novelty of this work is to follow the degradation mechanism of contaminants (VOCs/bacteria mixture) using pilot scale continuous photocatalytic reactor. Butane-2,3-dione (C<sub>4</sub>H<sub>6</sub>O<sub>2</sub>), Heptan-2-one (C<sub>7</sub>H<sub>14</sub>O) (i) and *Escherichia coli* (*E. coli*) (ii) were chosen as a VOCs (i) and bacteria strain (ii), specifically found in indoor air of food industries. The second novelty is to use a specific technology of textile fibers (TiO<sub>2</sub>, TiO<sub>2</sub>-Cu and TiO<sub>2</sub>-Ag), suitable for chemical/microbiological applications. The aim of this configuration is to provide a new and compact process, and no external UV lamps needed. To our knowledge, this is the first investigation on this combination (catalyst-reactor-semi-real conditions) which has been carried out at pilot scale.

**Table 1.** Oxidation technologies for VOC/bacteria removal (advantages and disadvantages).

Technologies	VOCs/bacteria	Reactor configuration		Technologies	
		batch reactor	continuous reactor	advantages	disadvantages
Photocatalysis [5,6,12-18]	bacteria	×	-	clean process	photocatalyst poisoning
	VOC	×	×		
	bacteria/VOC mixture	×	-	complete mineralization	

<b>Cold plasma</b> [7-9]	bacteria	×	-	high efficiency of reactive chemical species formation (at room temperature and atmospheric pressure)	by-products (e.g. Ozone, CO)
	VOC	-	×		low mineralization
	bacteria/VOC mixture	-	-		
× investigated, - not investigated					

## 2. Materials and methods

### 2.1. Polluted-contaminated air generation

Two targeted compounds like Butane-2,3-dione ( $C_4H_6O_2$ ) and Heptan-2-one ( $C_7H_{14}O$ ), belonging to ketone groups, were used. Butane-2,3-dione (99% purity) was purchased from Janssen Chimica, Belgium and Heptan-2-one of 98% purity, was supplied from Acros Organics, France. The objective of this study was to validate the photocatalysis process efficiency in a case closer to the real indoor air conditions. Butane-2,3-dione and Heptan-2-one were selected following the building air analysis campaign in a food industry (Brittany region of France- June 2019). The exposure limit values of Butane-2,3-dione is around  $11 \text{ mg}\cdot\text{m}^{-3}$  [28]. The polluted air flow was generated continuously by means of a syringe pump system (Kd Scientific Model 100, USA) in order to obtain a stable VOC concentration during the experiment (from 5 to  $20 \text{ mg}\cdot\text{m}^{-3}$ ). To create a VOCs/air mixture, two similar injection systems are used for each pollutant [29-31]. A static mixer at upstream ensures a proper mixing of air . The *Escherichia coli* (*E. coli* DSM 10198-0307-001) was obtained from Deutsche Sammlung von Mikroorganismen und Zellkulturen GmbH (DSMZ), Braunschweig, Germany. To test *E. coli* inactivation over time under a continuous photocatalytic reactor, aerosol/spray applications was performed via a nebulizer system. A set of valves and a flow controller (Bronkhorst In-Flow, France) were installed at the inlet of reactor (Figure 1. (a)). A maximum flow rate reached about  $12 \text{ m}^3\cdot\text{h}^{-1}$ . Humidity and

Temperature measurements were monitored via a specific sensor (Testo 445, Mönchaltorf, Switzerland). Two value of relative Humidity (% RH = 5% and % RH= 70%) of the effluent was investigated with using a packed column humidifier.

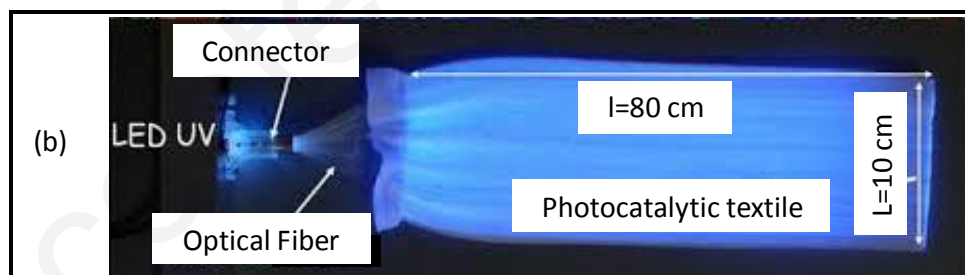
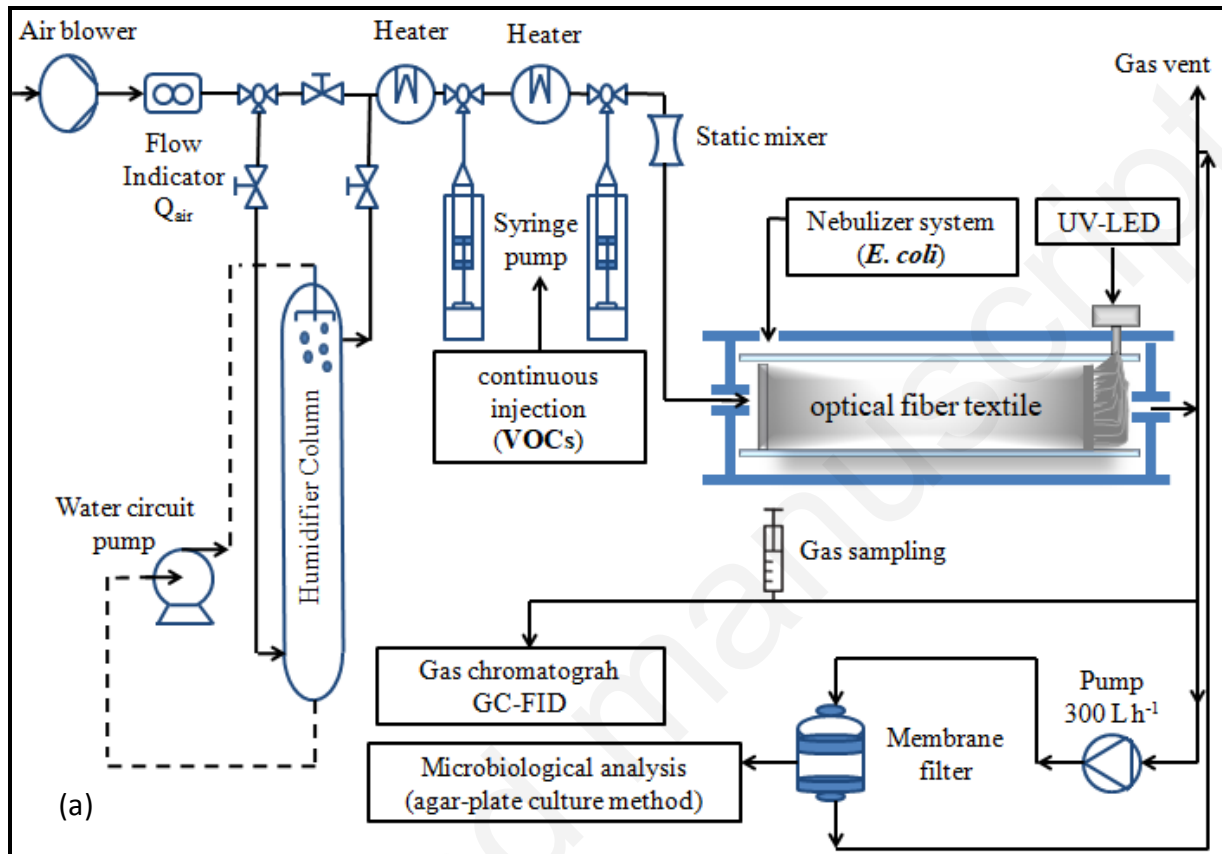


**Figure 1.** Schematic illustration of the used set-up for VOCs/Microorganisms inactivation via a new continuous photocatalytic reactor: (a) experimental set-up and (b) photocatalytic material.

## **2.2. Reactor design and catalyst form**

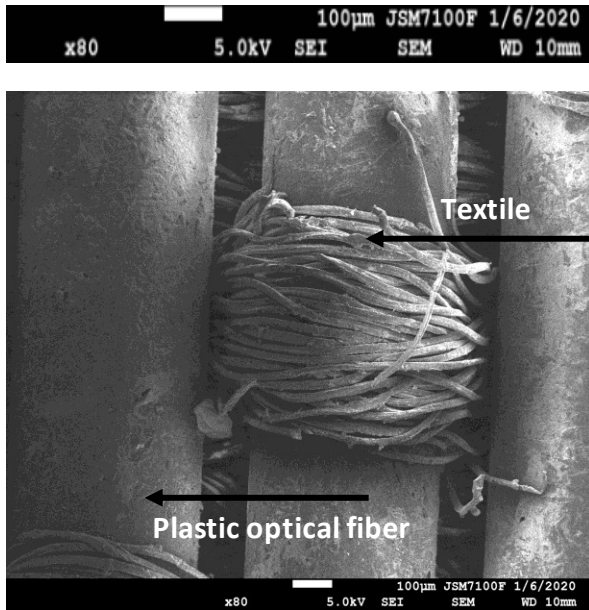
The pilot reactor, with its new configuration, was constructed to operate in photocatalytic mode using a novel catalytic material constructed with Copper (Cu)/Silver (Ag)-based optical fiber, double-sided optical fiber with a metal wire (Figure 2. (c)), as performed by Brochier Technologies Company (UVtex®) [32]. The characteristics of Optical Fiber (OF) are presented in Table 2. The optical fiber (Figure 2. (a)) is composed of (i) polymer fibers (polyester, Trévira CS™ fibres) and (ii) polyester fibers (polymethyl methacrylate, MMA CK-20 Eska™ fibres) and (iii) metallic wire. These elements are weaved following the Jacquard process meaning the interlacing, in a same plane, of fibers disposed in the direction of the chain (textile fiber) and some fibers disposed perpendicular to chain fibers, in the direction of the weft (optical fibers and metallic wire). These optical fibers have a mean diameter of 500  $\mu\text{m}$ , its core is made in polymethyl methacrylate resin with a 480  $\mu\text{m}$  mean diameter and covered with 10  $\mu\text{m}$  of thick fluorinated polymer [33]. In the absence of micro texturing the surface of the optical fibers, light is transmitted from to the end of the fabric. Since this fabric is intended to be the UV irradiation source, the whole surface of the textile must be bright. Micro texturing is a necessary treatment allowing a uniform light output across the surface of the optical fibers [34-35]. As described on our previous paper [39], the photocatalyst used is TiO<sub>2</sub> Degussa P25. The textile fibers, with/without metal wires (Cu/Ag), are coated with titanium dioxide in a bath of a concentrated aqueous suspension of TiO<sub>2</sub> (50 g L<sup>-1</sup>). The coating was carried out by dipping the optical fiber textile in the bath maintained at 70 °C during 1h. Then, the sample is dried during 1h at 70 °C. Luminous textile is coated by a first layer by silica to protect optical fiber aging. In absence of silica, the optical fiber could be attacked

by photocatalysis. However, silica is chosen because it allows the passage of UV, and it is not an organic compound therefore is not degraded by photocatalysis [36].

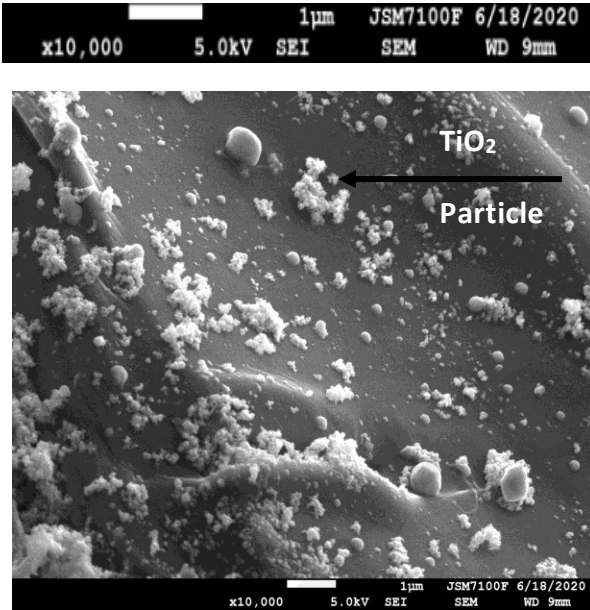
**Table 2.** Material specifications of photocatalyst.

metal/weaving	Surface illuminating	Allowable bending radius of OF	OF diameter
<ul style="list-style-type: none"> <li>- Textile wire of pure copper (Cu)</li> <li>- Textile wire with silver (0.4% Ag)</li> <li>- Bath coating of titanium dioxide (50 g L<sup>-1</sup>)</li> </ul>	Width (100 mm) Length (800 mm)	9 mm	500 μm

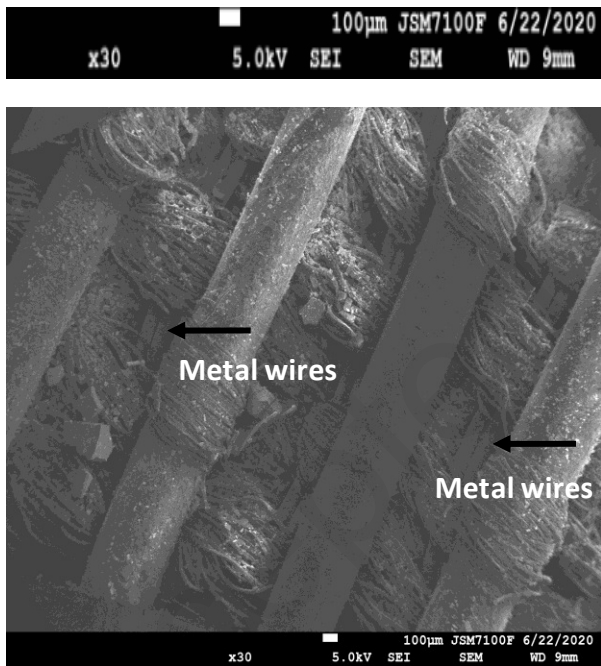
Figure 1. (a) shows of the image of the photocatalytic planar reactor. The reactor consists of a rectangular glass chamber with a length of 1000 mm and a square cross section up to 145 mm × 145 mm. Two glass plates are installed into the reactor and help to keep an attached catalyst textile (dimensions: plate thickness of 1 mm and 800 mm long). The distance between both textile catalysts may be modified to study gas gap effect on photocatalytic performance. Two UVA-LEDs (365 nm, UVA-LED intensity = 1.5 W m<sup>-2</sup>) are used to ensure a good distribution of radiation on the surface catalyst through fiber filaments, working in tangential flow with one pass (Figure 1. (b)). Figure 2. illustrates the structure of the textile fiber surface through SEM images of the photocatalytic material with and without TiO<sub>2</sub> and metal wires (Cu/Ag). The details of the surface texture characterization were analyzed by Scanning Electron Microscopy (SEM) using a JEOL JSM 7100 F microscope.



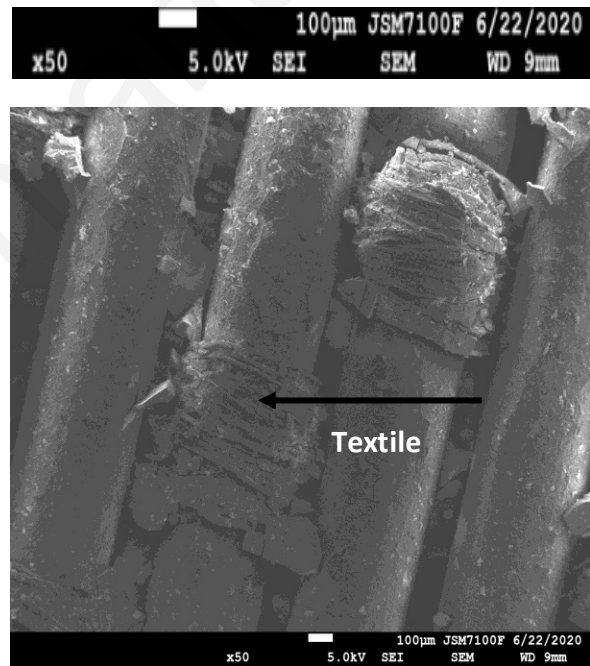
(a) Textile fiber without TiO<sub>2</sub>



(b) Textile fiber with TiO<sub>2</sub>



(c) Textile fiber with metal



(d) Textile fiber without metal

**Figure 2.** SEM images of the textile fiber surface: (a) and (b) SEM images of the textile fiber without and with TiO<sub>2</sub>, respectively ((a):\*80, (b):\*10000); (c) and (d) SEM images of the textile fiber with and without metal wires, respectively ((c):\*30, (d)\*50).

## **2.3. Photocatalytic analyses system**

### **2.3.1. VOCs monitoring**

Gas Chromatography (GC), fitted with a flame ionization detector (FID), was used to monitor the VOCs concentration at the reactor downstream. The analysis was carried out using a Clarus GC-500 chromatograph fitted with a 60 m × 0.25 mm polar DB-MS capillary column (film thickness, 0.25 μm). The inlet/outlet samples (500 μL) are injected via a gas syringe.

### **2.3.2. Microorganisms monitoring**

The performance of *E. coli* inactivation by each photo-catalyst was monitored over time by using agar-based culture method. Firstly, *E. coli* samples were collected on a polycarbonate membrane filter (Millipore, France) in a closed cassette 35 mm in diameter by using a membrane pump (KNF lab N86k18, France) with a 300 L.h<sup>-1</sup> flow (Figure 3). Secondly a desorption step of *E. coli* collected on membrane filter was realized using a sterile aqueous solution (Tween 80 0.01% Tryptone 0.1% H<sub>2</sub>O). The suspension consisting of bacteria was diluted in Tryptone medium and subsequently mixed thoroughly using a Vortex. 100 μL aliquots were plated on Tryptone Soya Agar (TSA) medium in Petri dishes. Then, all agar Petri dishes were incubated at 37°C for 24 h to allow bacterial growth.

## **3. Results and discussion**

First, the photocatalytic removal of Butane-2,3-dione, Heptan-2-one alone and *E. coli* have been studied separately. Then, the main novelty: mixture of VOCs and *E. coli* study at pilot scale, was also performed. The effect of all photo-catalysts on the efficiency of oxidation was evidenced under real operating conditions (VOCs/*E. coli* concentration, flow rate and humidity). Finally, the results observed are discussed (i)

in terms of photocatalytic (UV-LEDs) activities of TiO<sub>2</sub>-Cu/Ag used, (ii) in terms of the removal efficiencies (VOCs degradation/*E. coli* inactivation) and (iii) in terms of oxidation mechanisms.

### 3.1. Organic compounds treatment: Butane-2,3-dione & Heptan-2-one removal

#### 3.1.1. Effects of flow rate & VOC concentration

Some process parameters were modified during the photo-degradation study of VOCs like the initial VOCs concentration and the air flow rate. It is important to study the effect of operating parameters and to identify which factors influence the performance of oxidation step. Thus, operating parameters were monitored as (Eqs.1-2):

Butane-2,3-dione removal (%):

$$(\%) = \frac{([\text{Butane-2,3-dione}]_{\text{inlet}} - [\text{Butane-2,3-dione}]_{\text{outlet}}) \times 100}{[\text{Butane-2,3-dione}]_{\text{inlet}}} \quad (1)$$

• Heptan-2-one removal (%):

$$(\%) = \frac{([\text{Heptan-2-one}]_{\text{inlet}} - [\text{Heptan-2-one}]_{\text{outlet}}) \times 100}{[\text{Heptan-2-one}]_{\text{inlet}}} \quad (2)$$

Figure 3 and 4 show the evolution of Butane-2,3-dione removal according to  $[\text{Butane-2,3-dione}]_{\text{inlet}}$  and flow rate of VOCs/air, respectively. The experiments were performed ranging from 5 to 20 mg.m<sup>-3</sup> for different flow rates i.e. 2, 4, 8 and 12 m<sup>3</sup>.h<sup>-1</sup>. From figures 3 & 4, it was observed that for all photo-catalyst used i.e. TiO<sub>2</sub>, TiO<sub>2</sub>-Cu and TiO<sub>2</sub>-Ag, a similar oxidation behavior of removal efficiency vs inlet concentration was observed. However, a result shows that increasing the  $[\text{Butane-2,3-dione}]_{\text{inlet}}$  leads to a significant decrease in the catalytic activity of photo-catalyst and, potentially, limits its photocatalytic degradation. At a constant VOCs/air flow (equal to 2 m<sup>3</sup>.h<sup>-1</sup>) and in the case of TiO<sub>2</sub> study alone, the increase of the  $[\text{Butane-}$

2,3-dione]<sub>inlet</sub> from 5 to 20 mg.m<sup>-3</sup>, results in a decrease of the degradation rate from 66% to 38%. Our previous studies confirm this behavior for any other VOCs or groups of VOCs either at pilot or at industrial scale [37-41,25,26]. Therefore, photocatalysts containing metal wires e.g. Copper (Cu)/Silver (Ag) revealed a slight decrease compared to TiO<sub>2</sub> alone in terms of Butane-2,3-dione degradation performance but remains adequate for photocatalytic application. Similarly, it is readily seen in Figure 3 & 4 that the performance of degradation decreased with very high air flow (in our case 12 m<sup>3</sup>.h<sup>-1</sup>). This higher level of flow condition causes a decrease of the contact time between the Butane-2,3-dione and the active sites of catalyst and consequently impede the interesting adsorption/oxidation on the photocatalytic sites. For example, it has been noted that increasing VOCs/air flow from 2 to 12 mg.m<sup>-3</sup>, performance of oxidation showed a decrease from 55 to 33% in the case of TiO<sub>2</sub> study alone. Several studies confirm these experiment observations like Trichloromethane [42], inorganic compounds (e.g. Ammonia) [43], ketones (e.g. Heptan-2-one) [30], aldehydes (e.g. Butyraldehyde) [29] and related the slowdown in the performance. When VOCs inlet concentration is increased, due to the saturation and/or deactivation of the active sites by pollutants and /or oxidation by-products has been observed

This new configuration of material integrating photocatalyst (TiO<sub>2</sub>) and fiber optic lighting has also demonstrated its efficiency to remove the formaldehyde [33]. A good distribution of light on catalyst surface through fiber filaments improves the photocatalytic activity. A similar behavior (with concentration and flow rate) was also observed in the case of Heptan-2-one.

A comparative study of Heptan-2-one and Butane-2,3-dione behavior's was exhibited in our previous work (Glass Fiber Tissue as catalyst) [30] and the removal

efficiency would be much more remarkable in the case of Butane-2,3-dione which is why presently we are working with Butane-2,3-dione alone.

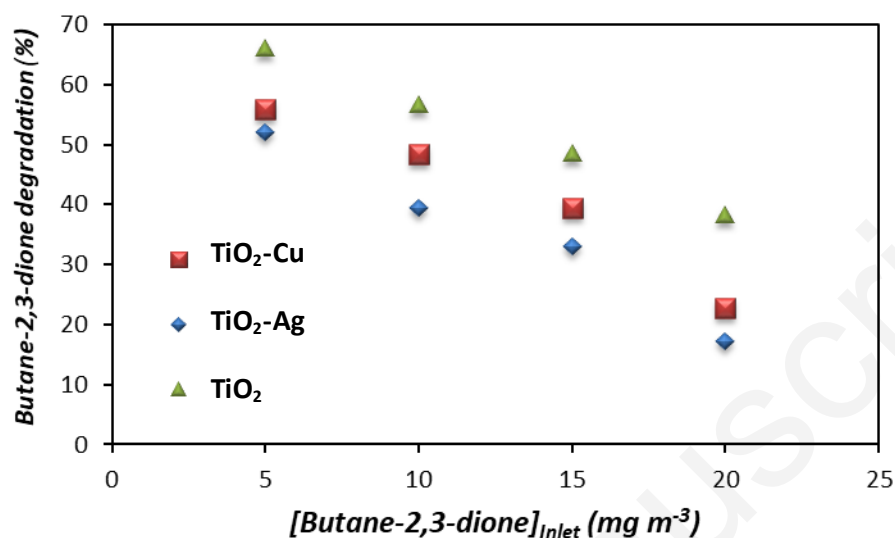


**Figure 3.** Variation of Butane-2,3-dione degradation (%) with inlet concentration ( $\text{mg m}^{-3}$ ) for different photo-catalysts ( $1 \text{ mg cm}^{-2}$   $\text{TiO}_2$ , 0.4% Ag, pure Cu). Operational conditions:  $T=20^\circ\text{C}$ , LED-UVA intensity=  $1.5 \text{ W m}^{-2}$ , Flow rate=  $2 \text{ m}^3 \cdot \text{h}^{-1}$ , dry air  $\sim 5\%$  of RH.

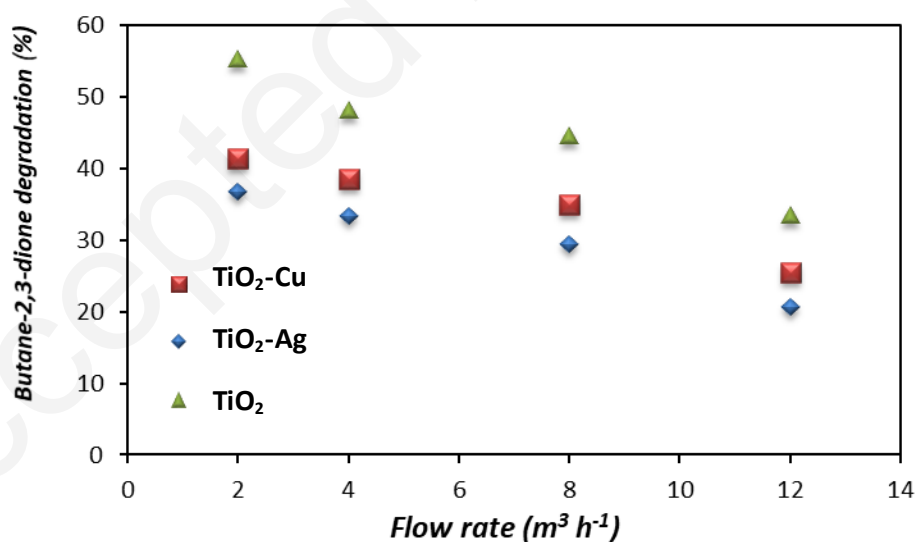


**Figure 4.** Variation of Butane-2,3-dione degradation (%) at different flow rates ( $\text{m}^3 \cdot \text{h}^{-1}$ ) with the three photo-catalysts ( $1 \text{ mg cm}^{-2}$   $\text{TiO}_2$ , 0.4% Ag, pure Cu). Operational conditions:  $T=20^\circ\text{C}$ , LED-UVA intensity=  $1.5 \text{ W m}^{-2}$ ,  $[\text{C}_4\text{H}_6\text{O}_2] = 10 \text{ mg} \cdot \text{m}^{-3}$ , dry air  $\sim 5\%$  of RH.

In order to improve the performance of this photocatalytic reactor and achieve higher levels of VOC removal, it is interesting to investigate (i) the effect of the number of the catalyst plates and (ii) the effect of space/air gap between the plates.

### **3.1.2. Effect of VOC mixing on removal efficiency**

In order to investigate the effect of (Butane-2,3-dione/Heptan-2-one) mixture on removal efficiencies, initial experiments were performed continuously with each VOCs alone and then with their equimolar mixture. Removal efficiencies were studied in the same operational conditions: input flow rate was set to  $2 \text{ m}^3 \cdot \text{h}^{-1}$  with  $\sim 5\%$  of humidity and initial concentration was  $20 \text{ mg} \cdot \text{m}^{-3}$  for each VOCs. The objective of this experiments study with the combination  $\text{TiO}_2$ /metallic wire was to validate the photocatalysis process efficiency for a simultaneous treatment (VOCs/bacteria) by using a specific catalyst exhibit promising antibacterial efficiency. Results of mixture study (with  $\text{TiO}_2$ -Ag and with  $\text{TiO}_2$ -Cu) are presented in Figure 5, interesting removal efficiency was obtained with  $\text{TiO}_2$ -Cu followed by  $\text{TiO}_2$ -Ag either for single or for mixture VOCs oxidation. First, it is readily seen (Figure 5) that oxidation performance of heptan-2-one remains low, removal efficiency  $\sim 19\%$  with  $\text{TiO}_2$ -Cu, compared to Butane-2,3-dione, removal efficiency  $\sim 41\%$  with  $\text{TiO}_2$ -Cu. As for mixture, a positive oxidation effect (under low intensity) is observed for Butane-2,3-dione experiments in the case of  $\text{TiO}_2$ -Cu and  $\text{TiO}_2$ -Ag but not obviously observed on Heptan-2-one. This trend clearly demonstrates that Heptan-2-one presents a long molecular chain ( $\text{C}_7\text{H}_{14}\text{O}$ ), harder to degrade via photocatalytic oxidation. Moreover, in our previous work, a classical configuration of the reactor was used with a  $\text{TiO}_2$ -GFT catalyst (Glass Fiber Tissue) and illuminated with external UV Lamp [30], oxidize by-products exhausts from  $\text{C}_4\text{H}_6\text{O}_2/\text{C}_7\text{H}_{14}\text{O}$  mixture are identified. Indeed, for a classical

configuration: the catalyst was illuminated with an external lamp. In this case, a glass annular reactor was used (2 concentric Pyrex cylinders, 100 cm length): the catalyst, Glass Fiber Tissue, is maintained on the inner reactor wall and the UV lamp (100 cm length) is placed in the inner concentric cylinder in order to have a homogeneous irradiation. The results showed that conventional by-products were created under photocatalytic treatment namely: Carbon dioxide, Acetone, Acetaldehyde, Acetic acid and Acid compounds (Formic acid, Propionic acid,...). In addition, the degradation pathway explaining what happens during the photocatalysis process has been added (Figure 6(a)). We suggest the following reactional scheme for Butane-2,3-dione/Heptan-2-one degradation, where Acetone ( $C_3H_6O$ ) and Propionic acid ( $C_3H_6O_2$ ) comes directly through Butanoic acid ( $C_4H_8O_2$ ), Pentanoic acid ( $C_5H_{10}O_2$ ) and Hexanoic acid ( $C_6H_{12}O_2$ ) and could dissociate into acetic acid ( $C_2H_4O_2$ ), acetaldehyde ( $C_2H_4O$ ) and Formic acid ( $CH_2O_2$ ). This last step (i) could be a common degradation pathway. Oxidation by-products (Figure 6(b)) were identified by Gas Chromatography coupled to Mass Spectrometry (GC-MS). Outlet oxidation reaction samples were concentrated on a Carbotrap (25 mL) and then removed by a thermal desorption unit coupled with GC-MS.

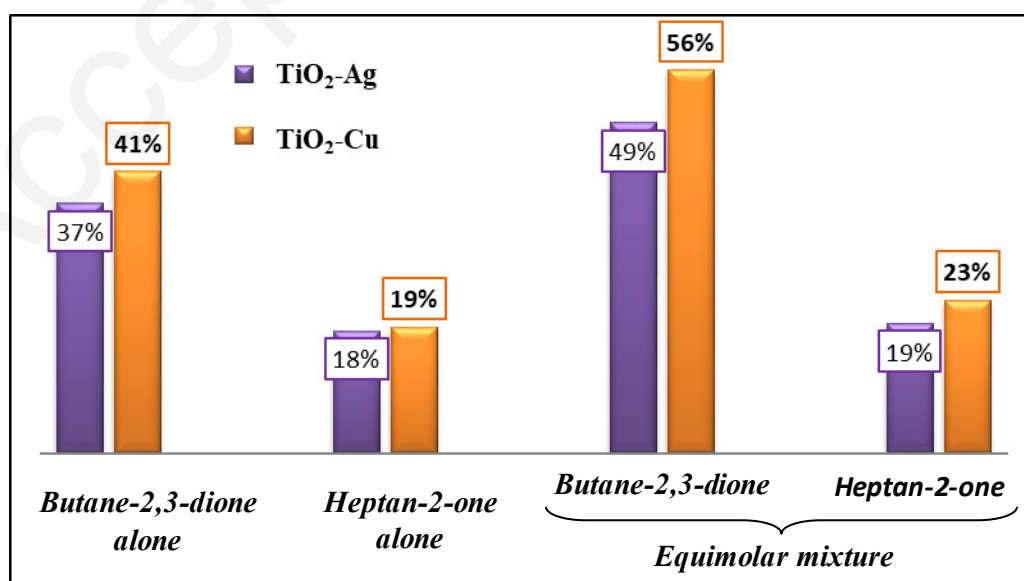


**Figure 5.** Variation of the removal efficiency of Butane-2,3-dione ( $C_4H_6O_2$ ) alone, Heptan-2-one ( $C_7H_{14}O$ ) alone and binary mixture via photocatalytic method. *Operational conditions:*  $T=20^\circ C$ ,  $Q= 2\ m^3.h^{-1}$ ,  $[Mixture]=[C_4H_6O_2]=[C_7H_{14}O]= 20\ mg.m^{-3}$ , dry air  $\sim 5\%$  of RH, catalyst:  $1\ mg\ cm^{-2}\ TiO_2$ ,  $0.4\%$  Ag, pure Cu.

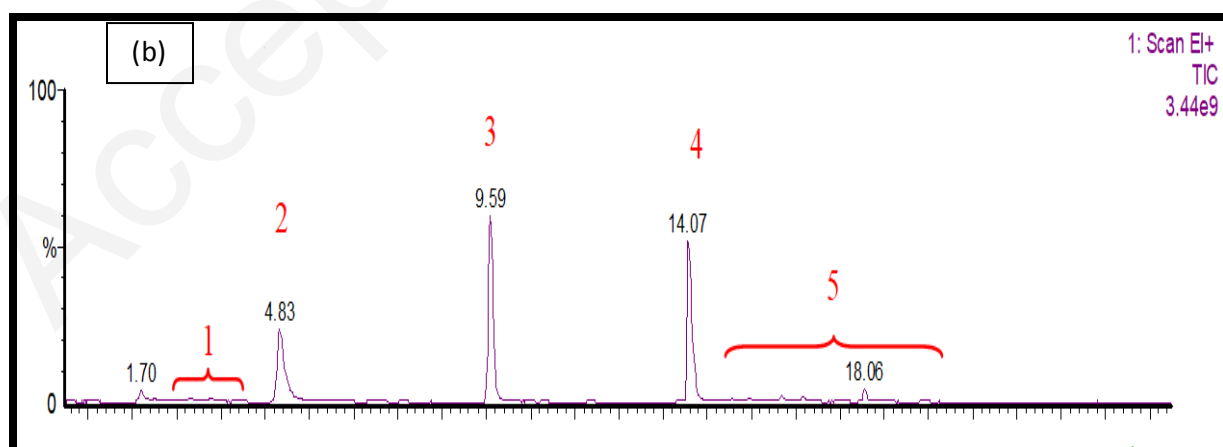
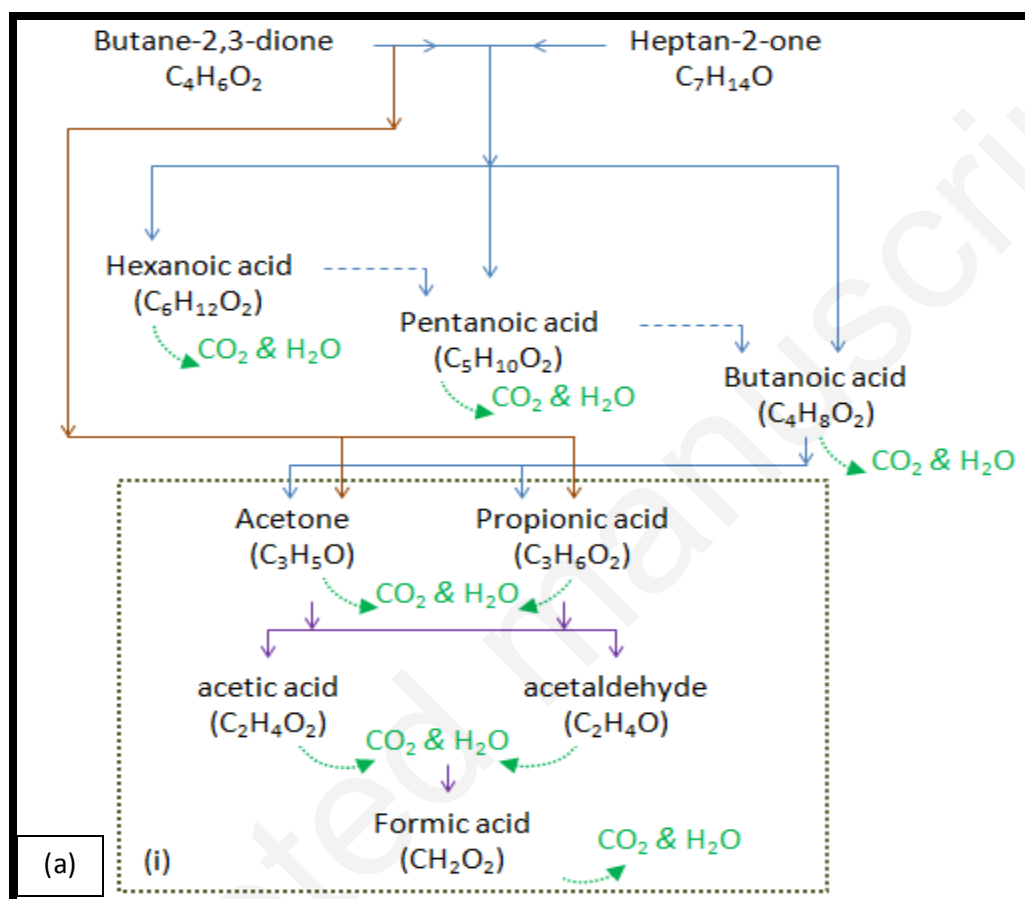


**Figure 6.** (a) Suggested reaction scheme of C<sub>4</sub>H<sub>6</sub>O<sub>2</sub>/C<sub>7</sub>H<sub>14</sub>O oxidation and (b) By-products identified by GC–MS following C<sub>4</sub>H<sub>6</sub>O<sub>2</sub>/C<sub>7</sub>H<sub>14</sub>O oxidation: (1) acetone and acetaldehyde, (2) Butane-2,3-dione, (3) Heptan-2-one, (4) acetic acid, (5) formic acid, propionic acid, butanoic acid, pentanoic acid, hexanoic acid and Heptane2,6-dione.

### 3.2. Bacterial inactivation: case of *Escherichia coli*

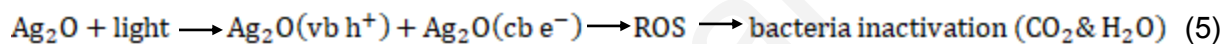
Before oxidation experiments via specific catalysts (TiO<sub>2</sub>-Cu, TiO<sub>2</sub>-Ag), a preliminary test (with TiO<sub>2</sub> alone) was conducted to verify its effectiveness. The experiment was performed in the same photocatalytic reactor, replacing a syringe pump system (VOCs) by a nebulizer system (*E. coli*), at a 1 m<sup>3</sup>.h<sup>-1</sup> input flow and *E. coli* initial concentration was 3 × 10<sup>3</sup> CFU.mL<sup>-1</sup> (Colony Forming Unit per milliliter). *Escherichia coli* can be encountered as air contaminant in food industry [44]. Bacterial inactivation under UV irradiation was then calculated as (Eq. 3):

$$A = \log(\text{CFU}_{\text{catalyst\_inlet}}) - \log(\text{CFU}_{\text{catalyst\_outlet}}) = \log\left(\frac{\text{CFU}_{\text{catalyst\_inlet}}}{\text{CFU}_{\text{catalyst\_outlet}}}\right) \quad (3)$$

where, A: antibacterial activity and CFU<sub>catalyst inlet</sub>, CFU<sub>catalyst outlet</sub> : number of CFU at the inlet and outlet of the photocatalytic reactor.

Results (Figure 7) showed that there is no inactivation of *E. coli* with TiO<sub>2</sub> alone during our experiments with continuous configuration. As for TiO<sub>2</sub>-Cu and TiO<sub>2</sub>-Ag, experimental results were presented in Figure 7. First, it is noticeable that *E. coli* inactivation increase when the photo-catalyst tissue is woven with TiO<sub>2</sub>-Ag and TiO<sub>2</sub>-Cu. Performance of *E. coli* inactivation under UVA light was estimated at around zero in the case of TiO<sub>2</sub> alone and in contrast to the other photo-catalysts, *E. coli* inactivation was 0.25 and 0.37 log CFU with TiO<sub>2</sub>-Ag and TiO<sub>2</sub>-Cu, respectively. This behavior indicates that the contact between Silver (Ag), Copper (Cu) and bacteria can play an important role to improve bactericidal activity [45]. It was shown by Rtimi

*et al.* that Silver and Copper accelerated bacterial inactivation due to its disinfecting properties [46]. The efficiency of *E. coli* inactivation under photocatalytic treatment is attributed to the oxidative damage mainly induced by the photogenerated reactive oxygen species/radicals ROS (e.g.  $O_2^{\bullet-}$ ,  $H_2O_2$  and  $HO^{\bullet}$ ) [47,48,19], produced by redox reactions between adsorbed species (e.g. water vapor and oxygen) and electrons/holes photo-generated. Xiong *et al.* and Joshi *et al.* showed that the light irradiation leads to generate the ROS and this may improve bacteria inactivation [48,19]. The reaction mechanism of Ag-NPs and Cu-NPs, under light, [50,51] can affect bacteria activity, as shown in Eqs. 4-5, under ROS (Eqs.6-9).



The synergistic mechanism for the photocatalytic inactivation of bacteria (*E. coli*) from indoor air in real condition (i) and the feasibility of simultaneous photo-oxidation of VOCs (Butane-2,3-dione & Heptan-2-one) is suggested in section 3.4 below. VOCs, VOCs by-products and *E. coli* suggested be adsorbing and/or oxidizing via ROS generated via Cu/Ag-doped  $TiO_2$ , under UVA irradiation. By heating Cu as a metal in air, Cu Oxide I and II are formed and consequently the formation of copper oxides can be formed during the fabric drying step following the step of the surface modified

of the semiconductor (in our case  $\text{TiO}_2$ ). As for Silver, Ag ions escape from Silver R.STAT® fibre, enter the bacterial wall; destroy its cellular structure thus preventing bacteria from developing and multiplying. In order to show the photocatalysis stability, the reusability of catalyst (with  $\text{TiO}_2\text{-Cu}$  and with  $\text{TiO}_2\text{-Ag}$ ) was studied (results on Figure 7). A stability of the performance of metal-fiber was confirmed after during the cyclic studies. In addition, experiment with (i) fibers alone without light and (ii) light alone without photocatalyst were also performed. Bacterial inactivation was negligible around 0.013 CFU (i) and  $< 0.01$  CFU (ii). We observed, in our previous work [52], a similar trend of bacterial removal efficiency in a batch reactor.

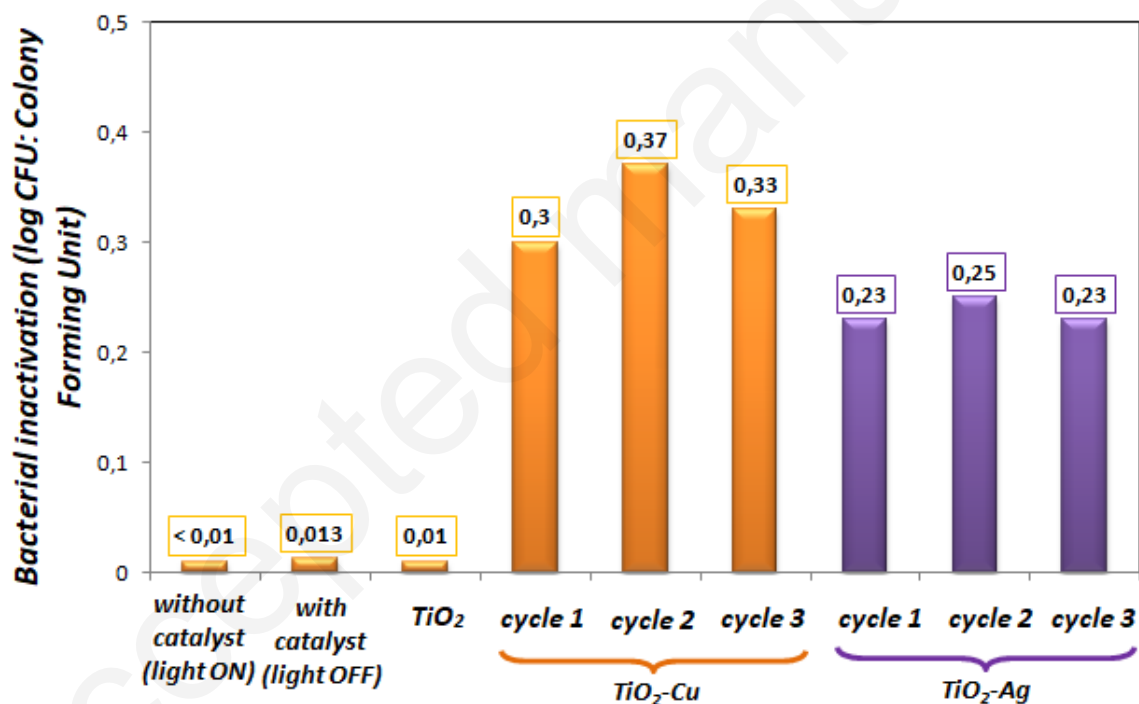


**Figure 7.** Bacterial inactivation (*E. coli*) via photocatalytic application with different photocatalysts:  $\text{TiO}_2$ ,  $\text{TiO}_2\text{-Cu}$  and  $\text{TiO}_2\text{-Ag}$ . Operational conditions:  $T=20^\circ\text{C}$ ,  $Q= 1 \text{ m}^3\cdot\text{h}^{-1}$ ,  $[\text{VOCs}]= 0 \text{ mg}\cdot\text{m}^{-3}$ ,  $[\text{E. coli}] = 3 \cdot 10^3 \text{ CFU}\cdot\text{ml}^{-1}$ , LED-UVA intensity=  $1.5 \text{ W m}^{-2}$ , dry air ~ 5% of RH.

### 3.3. Combination treatment: VOC/microorganisms removal

The removal of specific pollutants/microorganisms (as Butane-2,3-dione and *E. coli* in our case) is one of the principal objectives of indoor air treatment. In our study, the idea was to investigate, for the first time, the performance of photocatalytic application for simultaneous removal of VOCs and *E. coli* at pilot scale. Combination experiments were conducted with Butane-2,3-dione ( $10 \text{ mg.m}^{-3}$ ) and *E. coli* ( $3 \cdot 10^3 \text{ CFU.ml}^{-1}$ ) at dry conditions (air  $\sim 5\%$  of Relative Humidity, RH) with a flow rate around  $1 \text{ m}^3.\text{h}^{-1}$ . The pollutant degradation over time was monitored as well as the bacterial inactivation (Figure 8). First, three experiments were performed by using various catalysts ( $\text{TiO}_2$ ,  $\text{TiO}_2\text{-Ag}$  and  $\text{TiO}_2\text{-Cu}$ ). Results show an interesting efficiency in the case of  $\text{TiO}_2\text{-Ag}$  and  $\text{TiO}_2\text{-Cu}$ , indicating that these two metals oxides (in our case Silver and Copper) seem to be efficient for bacteria inactivation, which is attributable mainly to a damage of bacteria protein by the illumination of the photocatalyst surface [53, 50,51]. However, in the case of  $\text{TiO}_2\text{-Ag}$ , higher performance of Butane-2,3-dione removal (47%) was observed and in contrast to the *E. coli* inactivation was only around 0.25 CFU. As for  $\text{TiO}_2\text{-Cu}$ , results exhibit simultaneously (i) higher *E. coli* inactivation (1.27 CFU) and (ii) higher Butane-2,3-dione removal (52%). In our case, (i) this could be explained by the impact of by-products resulting from the degradation of VOCs on the behavior of *E.coli*. The LED-UVA intensity applied to the lamp is low (only  $1.5 \text{ W m}^{-2}$ ) and in view of this value (low-cost), (ii) a 52% VOC removal is an interesting result. Thus, a compromise must exist between the removal rate of the target molecule and the inactivation rate of bacteria with a metallic wire. On the other hand, the inactivation value was always zero via  $\text{TiO}_2$  alone, as shown in Figure 8. Thus, by comparing the inactivation efficiency obtained in the case of *E. coli* alone by photocatalytic process (Figure 7) to the results obtained in the case of *E. coli*/VOCs mixture (Figure 8). It is readily seen that the *E.*

*coli* inactivation is not influenced by the presence of VOCs. For example, we note that the inactivation of *E. coli* alone was around 0.25 log CFU (in the case of TiO<sub>2</sub>-Ag, Figure 7) and reaches 0.29 log CFU (in the case of *E. coli*/VOCs mixture, Figure 8). In this case, we can indicate also that the competition reactions of photo-catalyst between bacteria, VOCs and VOCs by-products are negligible.

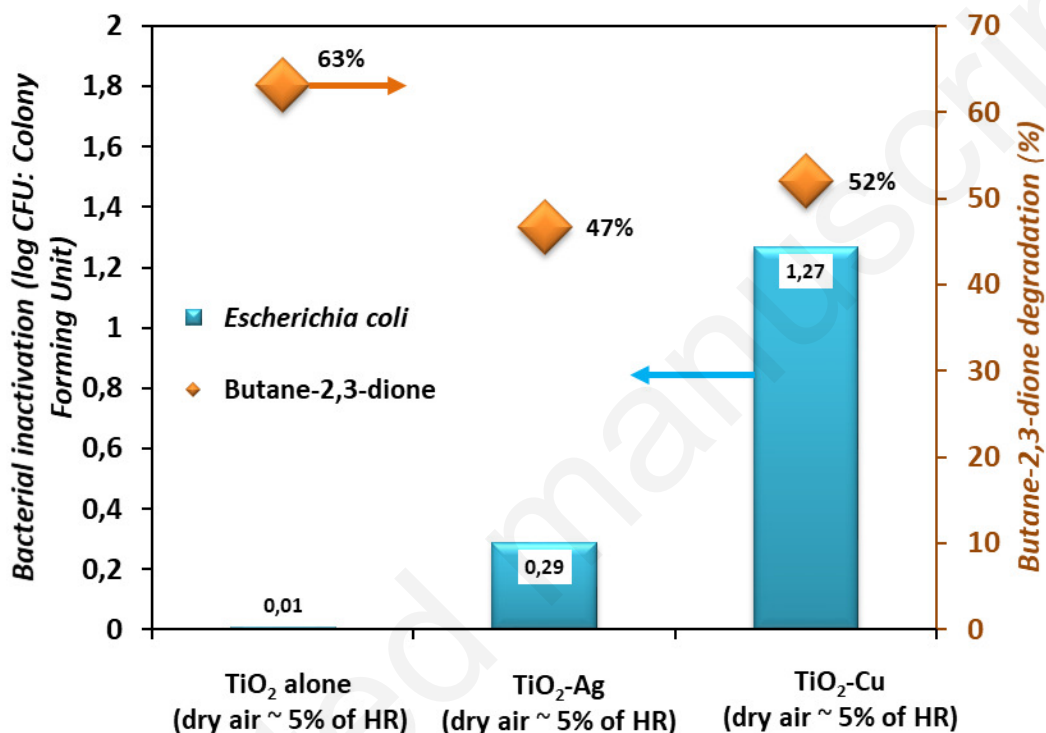


**Figure 8.** Bacterial inactivation (*E. coli*) and Butane-2,3-dione degradation using TiO<sub>2</sub>, TiO<sub>2</sub>-Ag and TiO<sub>2</sub>-Cu as catalyst, with dry air. *Operational conditions:*  $T=20^{\circ}\text{C}$ ,  $Q=1\text{ m}^3\cdot\text{h}^{-1}$ ,  $[E. coli]=3\cdot 10^3\text{ CFU}\cdot\text{m}^3$ ,  $[C_4H_6O_2]=10\text{ mg}\cdot\text{m}^{-3}$ ,  $\text{LED-UVA intensity}=1.5\text{ W m}^{-2}$ ,  $\text{RH}=5\%$ .

Moreover, *E. coli* inactivation kinetics as well as Butane-2,3-dione degradation (Figure 9) are seen to be more dependent on the humidity level of air stream. The same methodology as the first one (combined simultaneous Butane-2,3-dione and *E. coli* with dry input air) was conducted but with humid air. However, a result (in the case of TiO<sub>2</sub>-Cu) shows that the efficiency of removing/destroying contaminants

(under low UVA-LED light intensity) was lowered by increasing Relative Humidity from dry (~ 5% of RH) to wet air (~ 70% of RH). It is observed that when the water vapor amount is higher (~70%), the effect of the competitive adsorption/oxidation phenomena between VOCs, H<sub>2</sub>O and *E. coli* becomes more important which causes the VOCs/*E. coli* removal decrease [30,54-56]. However, indoor air in the food industry is usually humid (around 75-95% of humidity). As already noted that this study deals with indoor air treatment in simulated real conditions and which is why we studied a high level of humidity (~70%). Butane-2,3-dione removal and *E. coli* inactivation behavior were 52% and 1.27 log CFU (with dry flow), respectively and decreased to become 38% and 0.73 log CFU after the addition of water vapor into the photocatalytic reactor.

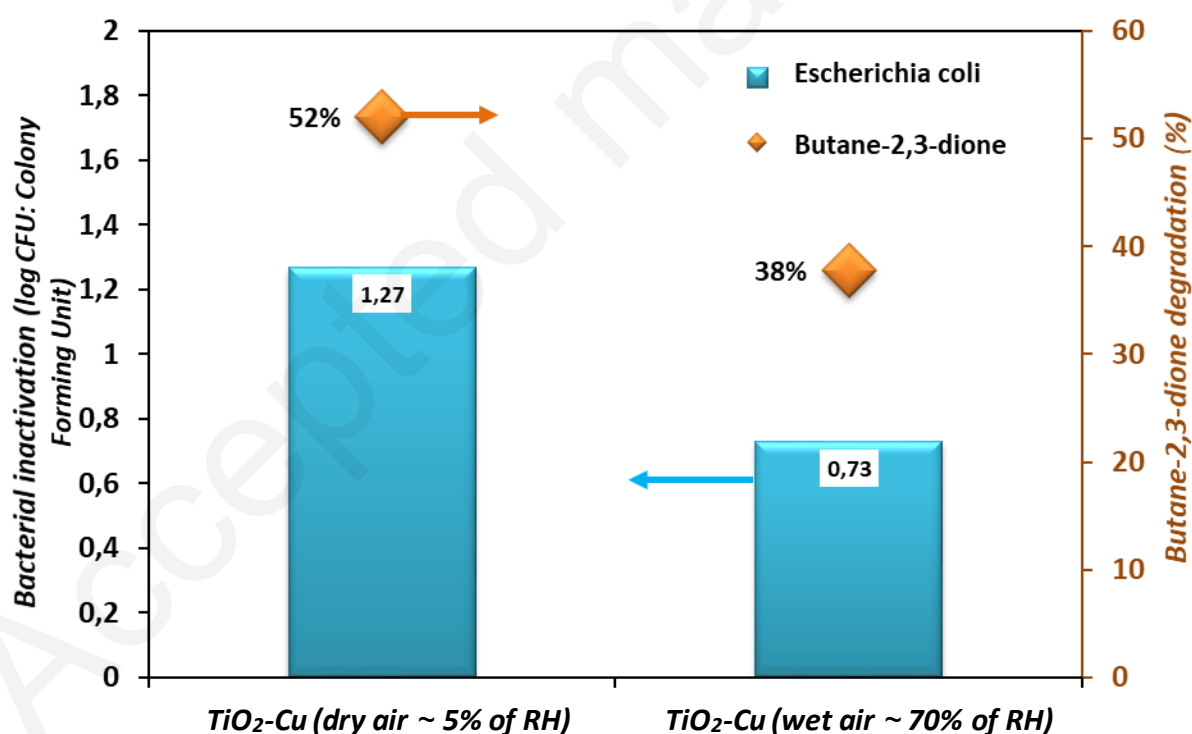


**Figure 9.** Bacterial inactivation (*E. coli*) and Butane-2,3-dione degradation using TiO<sub>2</sub>-Cu as catalyst, with dry and wet air. Operational conditions:  $T=20^{\circ}\text{C}$ ,  $Q=1\text{ m}^3\cdot\text{h}^{-1}$ ,  $[E. coli]=3\cdot 10^3\text{ CFU}\cdot\text{m}^3$ ,  $[C_4H_6O_2]=10\text{ mg}\cdot\text{m}^{-3}$ , LED-UVA intensity=  $1.5\text{ W m}^{-2}$ , RH= 5% and 70%.

### 3.4. Catalytic performance with real indoor air conditions

In order to confirm the good performance observed for destroying *Escherichia coli* (*E. coli*) under UVA-LED light in the presence of organic compounds (in our case Butane-2,3-dione), another experiences, with simulated real indoor air were performed. Here, a photocatalytic treatment with mixture of VOCs (Heptan-2-one) and *E. coli*, were performed. The photocatalytic reactor was continuously supplied with  $1 \text{ m}^3 \cdot \text{h}^{-1}$  of a dry air ( $\text{RH} \sim 5\%$ ). The initial concentrations were:  $3 \cdot 10^3 \text{ CFU} \cdot \text{ml}^{-1}$  of the *E. coli*,  $10 \text{ mg} \cdot \text{m}^{-3}$  of the Butane-2,3-dione and  $13.25 \text{ mg} \cdot \text{m}^{-3}$  of the Heptan-2-one. This value reflects the *Escherichia coli* concentration in real conditions (Building indoor air analysis campaign in a food industry (Brittany region of France- June 2019)). Regarding *E. coli*, with  $\text{TiO}_2\text{-Cu}$  under UVA-LED ( $1.5 \text{ W} \cdot \text{m}^{-2}$ ), it can be noted that the bacterial inactivation was around 0.37 for single oxidation (*E. coli* alone), reaches 1.27 and 1.77 for Butane-2,3-dione/*E. coli* and Heptan-2-one/*E. coli*, respectively (Figure 10). The reaction medium, combining simultaneous UVA-LED,  $\text{TiO}_2\text{-Copper}$ , VOCs and intermediate by-products, seem to be a powerful disinfectant for bacteria. About organic compounds behavior, a positive effect on oxidation performance was observed for both VOCs. Performance of VOCs degradation increases from 47% (Butane-2,3-dione) and 39% (Heptan-2-one), for single oxidation (VOCs alone), to 52% (Butane-2,3-dione) and 50% (Heptan-2-one) when both VOCs and bacteria mixed together. Indeed, the objective of this experiments study was to validate the photocatalysis process efficiency in a case closer to the real indoor air conditions where several pollutants/bacteria must be eliminated simultaneously and to see if there is always improvement of pollutants/bacteria removal in the case of mixing. Thus, in the best of cases (mixture target molecule/bacteria), a compromise must exist between the removal rate of the target molecule and the inactivation rate

of bacteria, and this is what was obtained during the photocatalysis, from which we concluded this promising technology for real applications.

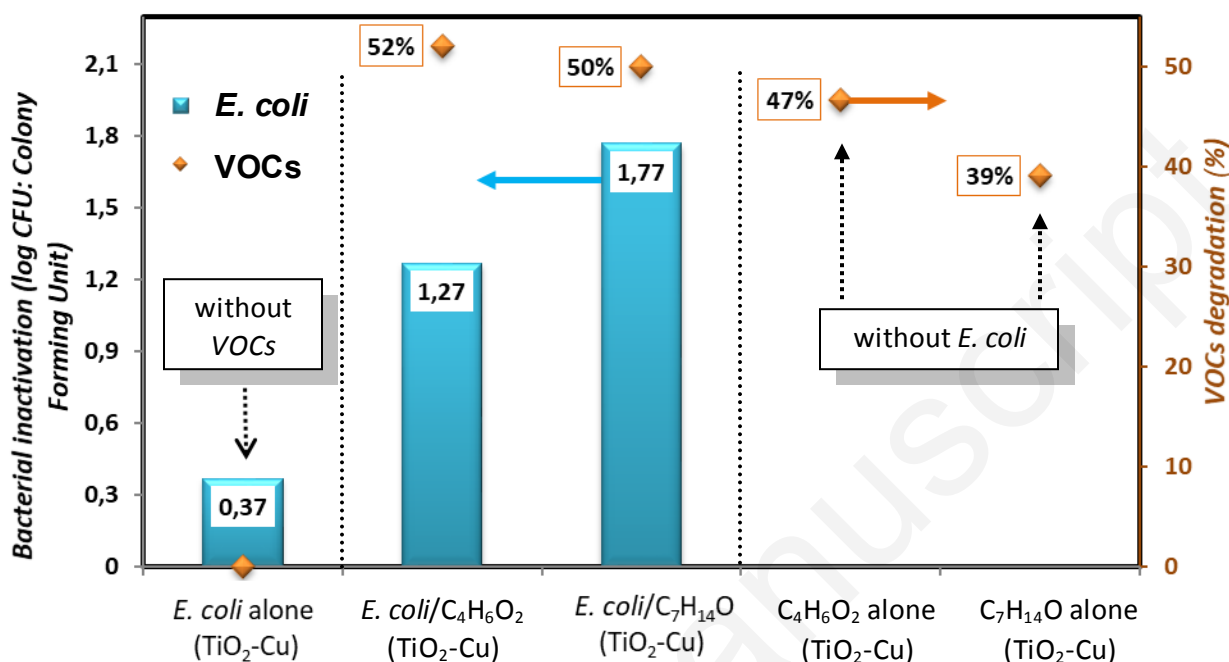


**Figure 10.** Bacterial inactivation (*E. coli*) and VOCs degradation using TiO<sub>2</sub>-Cu as catalyst.

Operational conditions:  $T=20^{\circ}\text{C}$ ,  $Q=1\text{ m}^3\text{ h}^{-1}$ ,  $[E. coli]=3\cdot 10^3\text{ CFU.ml}^{-1}$ ,  $[\text{VOCs}]=2.6\text{ ppm}$ ,

$\text{LED-UVA intensity}=1.5\text{ W m}^{-2}$ , dry air  $\sim 5\%$  of RH.

The experimental data obtained from all possible combinations namely: (a) TiO<sub>2</sub>-Cu/*E. coli*, (b) TiO<sub>2</sub>-Cu/Butane-2,3-dione/*E. coli* are summarized in Figure 10. It should be noted (Figure 10) from the *E. coli* behavior that the presence of Butane-2,3-dione and Heptan-2-one simultaneously with *Escherichia coli* significantly enhances their inactivation. The photocatalytic treatment is attributed to the activity between pollutant/bacteria and photogenerated reactive oxygen species/radicals ROS (e.g. O<sub>2</sub><sup>•-</sup>, H<sub>2</sub>O<sub>2</sub> and HO<sup>•</sup>) [44,45,19] (Figure 11), produced by redox reactions between adsorbed species (e.g. water vapor and oxygen) and electrons/holes photo-generated.

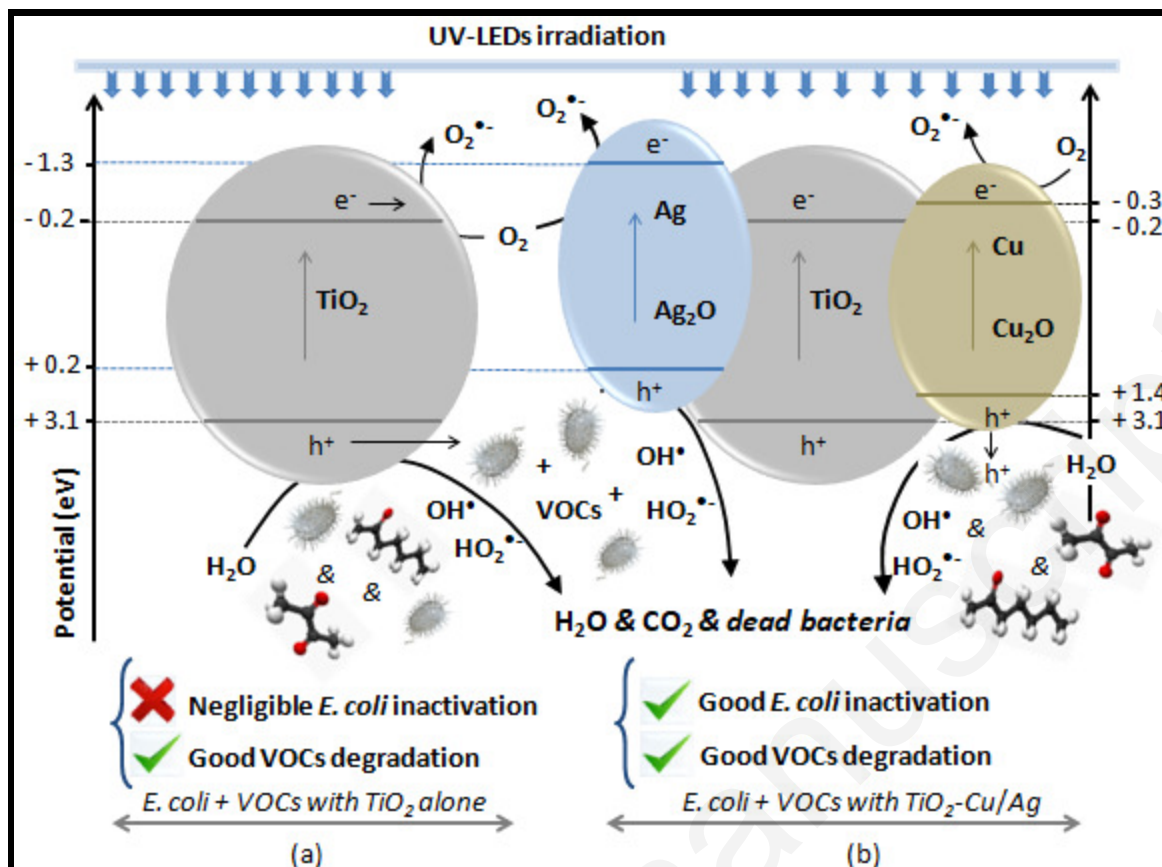


**Figure 11.** Suggested mechanism for *E. coli* inactivation and VOCs degradation under photocatalytic process: (a) *E. coli* + VOCs with  $\text{TiO}_2$  alone and (b) *E. coli* + VOCs with  $\text{TiO}_2$ -Cu/Ag.

#### 4. Conclusion

This new work aims to study the performance of photocatalytic application for the degradation/inactivation of contaminants (e.g. chemical and microbiological pollution) from indoor air (as Butane-2,3-dione/Heptan-2-one and *Escherichia coli* in our case). The selection of photo-catalyst that will be used simultaneously for VOCs and bacteria removals represents one of the key parameters towards efficiency of photocatalysis. Three new configurations of photo-catalyst ( $\text{TiO}_2$ ,  $\text{TiO}_2$ -Ag and  $\text{TiO}_2$ -Cu) were selected and their effect regarding oxidation performance was evaluated under a continuous system. Copper (Cu)/Silver (Ag) wires exhibit promising

antibacterial efficiency and can be considered as a potential new approach for the effective prevention of bacterial inactivation. In addition, competitive adsorption/oxidation phenomena between VOCs/H<sub>2</sub>O/*E. coli* can hamper the photocatalytic activity either for VOCs and/or for *E. coli*. Simultaneously to bacterial inactivation, VOCs removal was greatly enhanced, which adds value to this promising technology for real applications.

## References

- [1] C. Scotto, X. Fernandez, Olfactory pollution in urban environment: special case of odors in restaurants, *Atmospheric Pollution* N ° 234 April-June 2017.
- [2] Biological Pollutants' Impact on Indoor Air Quality, United States Environmental Protection Agency, January 2017, <https://www.epa.gov/indoor-air-quality-iaq/biological-pollutants-impact-indoor-air-quality> .
- [3] Institut nationale de recherche et de sécurité (INRS)-Fiche agents biologiques ED, 4414-décembre 2013.
- [4] Guidelines on air handling in the food industry-trends in Food Science & Technology, 17 (2006) 331-336.
- [5] T. Ramesh, B. Nayak, A. Amirbahman, Carl P. Tripp, S. Mukhopadhyay, Application of ultraviolet light assisted titanium dioxide photocatalysis for food safety: A review, *Innovative Food Science and Emerging Technologies*, 38, Part A (2016) 105-115.
- [6] Y. Huang, S.S. Hang Ho, Y. Lu, R. Niu, L. Xu, J. Cao, S. Lee, Removal of Indoor Volatile Organic Compounds via Photocatalytic Oxidation: A short Review and Porspect, *Molecules*, (2016) 21, 56.

- [7] F. Holzer, F.D. Kopinke, U. Roland, Non-thermal plasma treatment for the elimination of odorous compounds from exhaust air from cooking processes, *Chem. Eng. J.*, 334, 15 (2018) 1988-1995.
- [8] R. Thirumdas, C. Sarangapani, U.S. Annapure, Cold Plasma: A novel Non-Thermal Technology for Food Processing, *Food Biophysics*, 10 (2015) 1-11.
- [9] O. Karatum, M.A. Deshusses, A comparative study of dilute VOCs treatment in nonthermal plasma reactor, *Chem. Eng. J.*, 294 (2016) 308-315.
- [10] S. Alejandro-Martín, H. Valdés, M. H. Manero, C. A. Zaror, Catalytic Ozonation of Toluene Using Chilean Natural Zeolite: The Key Role of Brønsted and Lewis Acid Sites, *Catalysts*, 8(5) (2018) 211.
- [11] B. M. da Costa Filho, G. V. Silva, R. A.R. Boaventura, M. M. Dias, J.C.B. Lopes, V. J.P. Vilar, Ozonation and ozone-enhanced photocatalysis for VOC removal from air streams: Process optimization, synergy and mechanism assessment, *Science of The Total Environment*, 687 (2019) 1357-1368.
- [12] S. Rtimi, R. Sanjines, C. Pulgarin, J. Kiwi, Microstructure of Cu-Ag Uniform Nanoparticulate Films on Polyurethane 3D Catheters: Surface Properties, *ACS Appl. Mater. Interfaces*, 8, 1 (2016) 56-63.
- [13] R. Xie, D. Lei, Y. Zhan, B. Liu, Chi Him A. Tsang, Y. Zeng, K. Li, Dennis Y.C. Leung, H. Huang, Efficient photocatalytic oxidation of gaseous toluene over F-doped TiO<sub>2</sub> in a wet scrubbing process, *Chem. Eng. J.*, Available online 15 February 2019.
- [14] V. Héquet, C. Raillard, O. Debono, F. Thévenet, N. Locoge, L. Le Coq, Photocatalytic oxidation of VOCs at ppb level using a closed-loop reactor: The mixture effect, *Appl. Catal. B: Environ.*, 226 (2018) 473-486.

- [15] M. Malayeri, F. Haghghat, Chang-Seo Lee, Modeling of volatile organic compounds degradation by photocatalytic oxidation reactor in indoor air: A review, *Building and Environment*, 154 (2019) 309-323.
- [16] Z. Shayegan, F. Haghghat, Chang-Seo Lee, Photocatalytic oxidation of volatile organic compounds for indoor environment applications: Three different scaled setups, *Chem. Eng. J.*, 357 (2019) 533-546.
- [17] U. L. Rochetto, E. Tomaz, Degradation of volatile organic compounds in the gas phase by heterogenous photocatalysis with titanium dioxide/ultraviolet light, *Journal of the Air & Waste Management Association*, 65 (2015) 810-817.
- [18] Y. Boyjoo, H. Sun, J. Liu, V. K. Pareek, S. Wang, A review on photocatalysis for air treatment: From catalyst development to reactor design, *Chem. Eng. J.*, 310, Part 2 (2017) 537-559.
- [19] B. Joshi, C. Regmi, D. Dhakal, G. Gyawali, S. W. Lee, Efficient inactivation of *Staphylococcus aureus* by silver and copper loaded photocatalytic titanate nanotubes, *Progress in Natural Science: Materials International*, 28, 1 (2018) 15-23.
- [20] R. Gupta, N. KrishnaRao Eswar, J. M. Modak, G. Madras, Ag and CuO impregnated on Fe doped ZnO for bacterial inactivation under visible light, *Catalysis Today*, 300 (2018) 71-80.
- [21] T. D. Pham, B. K. Lee, D. Pham-Cong, Advanced removal of toluene in aerosol by adsorption and photocatalytic degradation of silver-doped TiO<sub>2</sub>/PU under visible light irradiation, *RSC Advances*, 6 (2016) 25346-25358.
- [22] G. Rao, K. S. Brastad, Q. Zhang, R. Robinson, Z. He, Y. Li, Enhanced disinfection of *Escherichia coli* and bacteriophage MS2 in water using a copper and

silver loaded titanium dioxide nanowire membrane, *Front. Environ. Sci. Eng.* (2016) 10(4): 11.

[23] W. Abou Saoud, A.A. Assadi, M. Guiza, A. Bouzaza, W. Aboussaoud, A. Ouederni, I. Soutrel, D. Wolbert, S. Rtimi, Study of synergetic effect, catalytic poisoning and regeneration using dielectric barrier discharge and photocatalysis in a continuous reactor: Abatement of pollutants in air mixture system, *Appl. Catal. B Environ.*, 213 (2017) 53-6.

[24] A. A. Assadi, A. Bouzaza, D. Wolbert, P. Petit, Isovaleraldehyde elimination by UV/TiO<sub>2</sub> photocatalysis: comparative study of the process at different reactors configurations and scales, *Environmental Science and Pollution Research*, 21 (2014) 11178-11188.

[25] A.A. Assadi, A. Bouzaza, D. Wolbert, Photocatalytic oxidation of Trimethylamine and Isovaleraldehyde in an annular reactor: Influence of the Mass Transfer and the relative humidity, *J. Photochem. Photobiol. A: Chem.*, 236 (2012) 61-69.

[26] A. A. Assadi, J. Palau, A. Bouzaza, J. Penya-Roja, V. Martinez-Soria, D. Wolbert, Abatement of 3-methylbutanal and trimethylamine with combined plasma and photocatalysis in a continuous planar reactor, *J. Photochem. Photobiol. A: Chem.*, 282 (2014) 1-8.

[27] M. Dhanasekar, V. Jenefer, Reshma B. Nambiar, S. Ganesh Babu, S. Periyar Selvam, B. Neppolian, S. Venkataprasad Bhat, Ambient light antimicrobial activity of reduced graphene oxide supported metal doped TiO<sub>2</sub> nanoparticles and their PVA based polymer nanocomposite films, *Materials Research Bulletin*, 97 (2018) 238-243.

[28] Valeurs limites d'exposition aux postes de travail 2016 : [www.suva.ch](http://www.suva.ch) , Edition: janvier 2016, Référence 1903.f

[29] W. Abou Saoud, A.A. Assadi, M. Guiza, A. Bouzaza, W. Aboussaoud, I. Soutrel, A. Ouederni, D. Wolbert, S. Rtimi, Abatement of ammonia and butyraldehyde under non-thermal plasma and photocatalysis: Oxidation processes for the removal of mixture pollutants at pilot scale, *Chem. Eng. J.*, 344 (2018) 165-172.

[30] W. Abou Saoud, A.A. Assadi, A. Kane, A.V. Jung, P. Le Cann, A. Gerard, A. Bouzaza, D. Wolbert, Integrated process for the removal of indoor VOCs from food industry manufacturing: elimination of Butane-2,3-dione and Heptan-2-one by cold plasma-photocatalysis combination, *J. Photochem.. Photobiol. A: Chem.*, 386 (2020) 112071.

[31] G. Costa, A.A. Assadi, S. Gharib-Abou Ghaida, A. Bouzaza, D. Wolbert, Study of butyraldehyde degradation and by-products formation by using a surface plasma discharge in pilot scale: Process modeling and simulation of relative humidity effect, *Chem. Eng. J.*, 307 (2017) 785-792.

[32] Brochier technologies, CNRS, UCBL1, INSERM, ENS, under number 2000384, Patent filed on 01/15/2020.

[33] P-A. Bourgeois, E. Puzenat, L. Peruchon, F. Simonet, D. Chevalier, E. Deflin, C. Brochier, C. Guillard, Characterization of a new photocatalytic textile for formaldehyde removal from indoor air, *Appl. Catal. B: Environ.* 128 (2012) 171-178.

[34] C. Brochier, D. Malhomme, E. Deflin, Brevet 2007, Nappe textile présentant des propriétés dépolluantes par photocatalyse, under number FR2910341, 27/06/2008 (A1) and FR2910341, 06/02/2009 (B1).

[35] C. Brochier, E. Deflin, Brevet N° WO 2008/062141, Complexe éclairant verrier. 2008, FR2908864 (A1) 2008-0523.

[36] C. Indermühle, E. Puzenat, F. Simonet, L. Peruchon, C. Brochier, C. Guillard, Modelling of UV optical ageing of optical fibre fabric coated with TiO<sub>2</sub>, Appl. Catal. B: Environ. 182 (2016) 229-235.

[37] A. Bouzaza, C. Vallet, A. Laplanche, Photocatalytic degradation of some VOCs in the gas phase using an annular flow reactor: determination of the contribution of mass transfer and chemical reaction steps in the photo-degradation process, J. Photochem. Photobiol. A: Chem., 177, 2-3 (2006) 212-217.

[38] A.A. Assadi, A. Bouzaza, I. Soutrel, P. Petit, K. Medimagh, D. Wolbert, A study of pollution removal in exhaust gases from animal quartering centers by combining photocatalysis with surface discharge plasma: from pilot to industrial scale, Chem. Eng. Process., 111 (2017) 1-6.

[39] A.A. Assadi, S. Loganathan, N. Tri Phuong, S. Gharib-Abou Ghaida, A. Bouzaza, N. Tuan Anh, D. Wolbert, Pilot scale degradation of mono and multi volatile organic compounds by surface discharge plasma/TiO<sub>2</sub> reactor: investigation of competition and synergism, J. Hazard. Mater., 357 (2018) 305-313.

[40] T. Zadi, M. Azizi, N. Nasrallah, D. Wolbert, S. Rtimi, A. A. Assadi, Indoor air treatment of refrigerated food chambers with synergetic association between cold plasma and photocatalysis: Process performance and photocatalytic poisoning, Chem. Eng. J., 382 (2020) 122951.

[41] S. Gharib-Abou Ghaida, A.A. Assadi, G. Costa, A. Bouzaza, D. Wolbert, Association of surface dielectric barrier discharge and photocatalysis in continuous

reactor at pilot scale: Butyraldehyde oxidation, by-products identification and ozone valorization, *Chem. Eng. J.*, 292 (2016) 276-283.

[42] T. Zadi, A.A. Assadi, N. Nasrallah, R. Bouallouche, P.N. Tri, A. Bouzaza, M.M. Azizi, R. Maachi, D. Wolbert, Treatment of hospital indoor air by a hybrid system of combined plasma with photocatalysis: Case of trichloromethane, *Chem. Eng. J.*, 349 (2018) 276-286.

[43] G. Maxime, A.A. Assadi, A. Buzaza, D. Wolbert, Removal of gas-phase ammonia and hydrogen sulfide using photocatalysis, nonthermal plasma, and combined plasma and photocatalysis at pilot scale, *Environ. Sci. Pollut. Res.*, 21 (2014) 13127-13137.

[44] P. Whyte, J.D. Collins, K. McGill, C. Monahan, H. O'mahony, Distribution and Prevalence of Airborne Microorganisms in Three Commercial Poultry Processing Plants, *J. Food Prot.* (2001) 64 (3): 388-391.

[45] A. A Assadi, A Bouzaza, D Wolbert, P Petit, Isovaleraldehyde elimination by UV/TiO<sub>2</sub> photocatalysis: comparative study of the process at different reactors configurations and scales, *Environmental Science and Pollution Research* 21 (2014), 11178-11188

[46] S. Rtimi, D. D. Dionysiou, S. C. Pillai, J. Kiwi, Advances in catalytic/photocatalytic bacterial inactivation by nano Ag and Cu coated surfaces and medical devices, *Appl. Catal. B: Environ.*, 240 (2019) 291-318.

[47] T. Verdier, M. Coutand, A. Bertron, C. Roques, Antibacterial Activity of TiO<sub>2</sub> Photocatalyst Alone or in Coatings on *E. coli*: The Influence of Methodological Aspects, *Coatings*, 4(3) (2014) 670-686.

- [48] L. Xiong, F. Yang, L. Yan, N. Yan, X. Yang, M. Qiu, Y. Yu, Bifunctional photocatalysis of TiO<sub>2</sub>/Cu<sub>2</sub>O composite under visible light: Ti<sup>3+</sup> in organic pollutant degradation and water splitting, *J. Phys. Chem. Solids*, 72, 9 (2011) 1104-1109.
- [49] A.A. Assadi, A. Bouzaza, D. Wolbert, Kinetic modeling of VOC photocatalytic degradation using a process at different reactor configurations and scales, *International Journal of Chemical Reactor Engineering* 14 (1), (2016) 395-405
- [50] M. Abidi, A.A. Assadi, A. Bouzaza, A. Hajjaji, B. Bessais, S. Rtimi, Photocatalytic indoor/outdoor air treatment and bacterial inactivation on Cu<sub>x</sub>O/TiO<sub>2</sub> prepared by HiPIMS on polyester cloth under low intensity visible light, *Appl. Catal. B: Environ.*, 259 (2019) 118074.
- [51] J. L. Liu, Z. Luo, S. Bashir, A progressive approach on inactivation of bacteria using silver-titania nanoparticles, *Biomater. Sci.*, 1 (2013) 194-201.
- [52] M. Abidi, A Hajjaji, A. Bouzaza, K Trablesi, H. Makhlouf, S. Rtimi, A.A. Assadi, B. Bessais Simultaneous removal of bacteria and volatile organic compounds on Cu<sub>2</sub>O-NPs decorated TiO<sub>2</sub> nanotubes: competition effect and kinetic studies, *J. Photochem.. Photobiol. A: Chem.*, 400 (2020) 112722.
- [53] H. Li, Q. Cui, B. Feng, J. Wang, X. Lu, J. Weng, Antibacterial activity of TiO<sub>2</sub> nanotubes: influence of crystal phase, morphology and Ag deposition, *Appl. Surf. Sci.*, 284 (2013) 179-183.
- [54] W. Abou Saoud, A. A. Assadi, M. Guiza, S. Loganathan, A. Bouzaza, W. Aboussaoud, A. Ouederni, S. Rtimi, D. Wolbert, Synergism between non-thermal plasma and photocatalysis: Implications in the post discharge of ozone at a pilot scale in a catalytic fixed-bed reactor, *Appl. Catal. B: Environ.*, 241(2019) 227-235.

[55] H. L. Huang, M. G. Lee, J. H. Tai, Controlling Indoor Bioaerosols Using a Hybrid System of Ozone and Catalysts, *Aerosol and Air Quality Research*, *Aerosol and Air Quality Research*, 12: (2012) 73-82.

[56] B. Sánchez, M. Sánchez-Muñoz, M. Muñoz-Vicente, G. Cobas, R. Portela, S. Suárez, A. E. González, N. Rodríguez, R. Amils, Photocatalytic elimination of indoor air biological and chemical pollution in realistic conditions, *Chemosphere*, 87, 6 (2012) 625-630.

Accepted manuscript